



Supporting Online Material for
**Splitting of the 520-Kilometer Seismic Discontinuity and Chemical
Heterogeneity in the Mantle**

Ashima Saikia,* Daniel J. Frost, David. C. Rubie

*To whom correspondence should be addressed. E-mail: ashima.saikia@uni-bayreuth.de

Published 14 March 2008, *Science* **319**, 1515 (2008)
DOI: 10.1126/science.1152818

This PDF file includes:

Materials and Methods
Tables S1 to S4
References

Supporting online material

Materials and Methods

Glass starting compositions for garnet synthesis experiments are given in Table S1. Multianvil experiments were performed using Cr₂O₃-doped MgO octahedra of 10 mm edge length in combination with tungsten carbide cubes with 4 mm truncation edge lengths. A LaCrO₃ heater was employed and a W3%Re-W25%Re thermocouple was inserted axially into the furnace inside an alumina thermocouple sleeve. The capsule was made from 1 mm diameter Re wire that was spark eroded to form four 0.3mm diameter sample chambers. Each of the three sample chambers was loaded with a garnet/CaSiO₃ composition of different garnet Al/Si ratio. One sample chamber contained a (Fe,Mg)₂SiO₄ olivine starting material with a Fe/(Fe+Mg) ratio chosen such that it would crystallize as ringwoodite + magnesiowüstite + stishovite at high pressure and temperature. A 0.025 mm thick Re disk covered the upper surface of the sample capsule. Experiments were compressed in a 1000 tonne press and then heated for at least 24 hours to equilibrate the samples. After quenching by turning off the furnace power, the experiment was decompressed over at least 15 hours at room temperature. Recovered samples were mounted in epoxy resin and polished on the surface that was perpendicular to the axial direction of the furnace and close to the thermocouple. Samples were analyzed with electron microprobe to determine phase compositions and Raman spectroscopy was employed for phase identification. In most garnet samples a 5 wt % B₂O₃ was added as a flux. This dramatically increased the rate of reaction at 1600°C and 1400 °C but reaction rates at 1200 °C were far too slow for equilibrium to be achieved on feasible time scales. Some recovered samples were made into petrographic thin sections and ion thinned for analysis with transmission electron microscopy. Electron energy loss spectroscopy found no detectable boron in the recovered mineral phases.

Pressure calibration

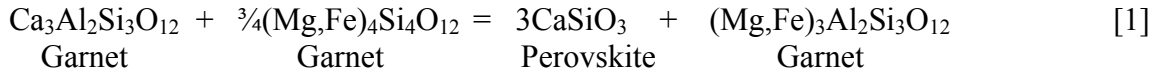
One olivine sample was included in each experiment as a pressure calibrant. Pressure was determined from the Mg₂SiO₄-Fe₂SiO₄ phase diagram using the field of coexistence between (Fe,Mg)₂SiO₄ ringwoodite and (Mg,Fe)O magnesiowüstite plus stishovite. This divariant region extends from approximately 16 GPa to 23 GPa with the Fe content of both ringwoodite and magnesiowüstite (when coexisting with stishovite) decreasing with increasing pressure. This reaction has been well studied (1,2). The Fe/(Fe+Mg) ratio of ringwoodite for example decreases by approximately 10 % per GPa. Given that we can determine this ratio with an accuracy of approximately 1%, this gives us a precision in pressure determination of 0.1 GPa. A previous study has shown that the bulk Fe concentration of magnesiowüstite can be apparently high if ferric Fe is present (2), therefore, we calculate the pressure using the ringwoodite Fe concentration and use phase relations previously determined at a similar oxygen fugacity (1). The relative pressure errors, shown in table 1, are calculated using the mismatch between the Fe content of ringwoodite and magnesiowüstite analyzed and that on the phase diagram (1). The

absolute error in pressure depends on determinations of end member phase transitions used to construct the existing Mg₂SiO₄-Fe₂SiO₄ phase diagram, which are difficult to assess but could be up to 0.5 GPa. Our study, however, relies much more on the high precision of pressures determined relative to the Mg₂SiO₄-Fe₂SiO₄ phase diagram, rather than accuracy in absolute pressure.

In some instances magnesiowüstite grains were too small to obtain reliable analyses and so pressures were determined using the ringwoodite Fe content alone. In other instances (Fe,Mg)₂SiO₄ starting compositions were poorly chosen in terms of their Fe/(Fe+Mg) ratios such that in the experiment the compositions crystallized as single phase ringwoodite and not within the divariant two phase region. In these cases pressure was determined from the oil pressure of the multianvil experiment. In experiments where the pressure was measured, the determined pressure shows an excellent relationship with the multianvil oil pressure. The relative uncertainty in using this calibration curve is approximately 0.5 GPa. As stated above, the absolute uncertainty depends on end member pressure determinations, which could be as great as 0.5 GPa. The thermodynamic data used to calculate the wadsleyite to ringwoodite transition are internally consistent with the same phase diagram used to calculate the pressure in the experiments (1-3).

Thermodynamic model

The exsolution of CaSiO₃ perovskite can be described by the reaction



where we implicitly assume that Ca is mixing only on the dodecahedral site. Ignoring Fe for the moment the equilibrium constant for this reaction is.

$$K = \frac{\left[a_{\text{Mg}_3\text{Al}_2\text{Si}_3\text{O}_{12}}^{\text{Gt}} a_{\text{CaSiO}_3}^{\text{Pv}} \right]^3}{\left[a_{\text{Ca}_3\text{Al}_2\text{Si}_3\text{O}_{12}}^{\text{Gt}} a_{\text{Mg}_4\text{Si}_4\text{O}_{12}}^{\text{Gt}} \right]^4} \quad [2]$$

The activity of CaSiO₃ is unity but the activities of the garnet components are described by:-

$$a_{\text{Mg}_4\text{Si}_4\text{O}_{12}}^{\text{Gt}} = \gamma_{\text{Mg}_4\text{Si}_4\text{O}_{12}}^{\text{Gt}} \left(X_{\text{Maj}}^{\text{oct}} \right) \left(X_{\text{Mg}}^{\text{dodec}} \right)^3 \quad [3]$$

$$a_{\text{Ca}_3\text{Al}_2\text{Si}_3\text{O}_{12}}^{\text{Gt}} = \gamma_{\text{Ca}_3\text{Al}_2\text{Si}_3\text{O}_{12}}^{\text{Gt}} \left(1 - X_{\text{Maj}}^{\text{oct}} \right) \left(X_{\text{Ca}}^{\text{dodec}} \right)^3 \quad [4]$$

$$a_{Mg_3Al_2Si_3O_{12}}^{Gt} = \gamma_{Mg_3Al_2Si_3O_{12}}^{Gt} (1 - X_{Maj}^{oct}) (X_{Mg}^{dodec})^3 \quad [5]$$

Where

$$X_{Maj}^{oct} = \left(\frac{2 - nAl}{2} \right) \quad [6]$$

$$X_{Mg}^{dodec} = \left(\frac{3 - nCa - nFe}{3} \right) \quad [7]$$

$$X_{Ca}^{dodec} = \left(\frac{nCa}{3} \right) \quad [8]$$

Here nAl , nCa and nFe are element proportions in garnet based on 12 oxygen formula units and γ is the activity coefficient. Si and Mg are therefore assumed to be locally ordered on the octahedral site. At equilibrium:-

$$\Delta G_{P,T}^0 = -RT \ln \frac{[a_{Mg_3Al_2Si_3O_{12}}^{Gt}]}{[a_{Ca_3Al_2Si_3O_{12}}^{Gt}] [a_{Mg_4Si_4O_{12}}^{Gt}]^3} \quad [9]$$

where $\Delta G_{P,T}^0$ is the standard Gibbs free energy change of the pure components at pressure and temperature, which can be simply described in terms of entropy, enthalpy and volume changes by,

$$\Delta G_{P,T}^0 = \Delta H - T\Delta S + P\Delta V \quad [10]$$

The terms in equation [7] were determined by fitting $-RT \ln K$ as a function of P and T. The activity coefficients (γ) were first determined using a 4 component symmetric solution model that included terms for the non ideality of majorite mixing. However, all majorite terms, which were refined in the fitting, were very small and were therefore ignored. A ternary symmetric solution model was then used that accounted for non ideality resulting from Mg, Ca and Fe mixing only on the dodecahedral site i.e.

$$RT \ln \gamma_{Mg_3Al_2Si_3O_{12}}^{Gt} = X_{Ca}^2 W_{MgCa} + X_{Fe}^2 W_{MgFe} + X_{Ca} X_{Fe} (W_{MgCa} + W_{MgFe} - W_{CaFe}) \quad [11]$$

$$RT \ln \gamma_{Ca_3Al_2Si_3O_{12}}^{Gt} = X_{Mg}^2 W_{MgCa} + X_{Fe}^2 W_{CaFe} + X_{Mg} X_{Fe} (W_{MgCa} + W_{CaFe} - W_{MgFe}) \quad [12]$$

where W are Margules interaction parameters. Note that we use mole fractions of cations on the dodecahedral site to calculate the excess free energy, which implies that the excess free energy arising from Mg-Ca interaction is not decreased by adding majorite. The following values were chosen guided by the literature (4,5).

$$W_{MgFe} = 300 \text{ Joules} \quad [13]$$

$$W_{CaFe} = 2000 \text{ Joules} \quad [14]$$

Although many studies show the pyrope-grossular solid solution to have significant asymmetric excess enthalpy, entropy and volume properties, extrapolations of the many published models to pressures in excess of 20 GPa and 1873K yield wildly disparate activity coefficients. We have no option but to treat W_{MgCa} as an adjustable parameter but the range of Ca contents covered by our data makes an asymmetric fit unconstrained and unnecessary for our purposes. Therefore we refine symmetric terms for W_{MgCa} but constrain them to vary over a range predefined from literature values to get,

$$W_{MgCa} = 8000 + 300P \text{ Joules} \quad [15]$$

where P is in GPa. The refinement gives

$$\Delta G_{p,T}^0 = 140763(17000) + 26.8(8.0)T - 12560(600)P \quad [16]$$

with T in K and P in GPa. The volume change of equation 1 is therefore $-12.5(6) \text{ cm}^3 \text{ mol}^{-1}$ which is very reasonable given the volumes and equation of state properties of the phases involved (see next section). A reciprocal solution model was also attempted but it did not significantly improve the fit.

Elasticity calculation

Density and S-wave velocity at high pressure and temperature were estimated using the data in table S3. Density and the elastic moduli were first calculated at 1 bar and high temperature then extrapolated along individual mineral adiabats using third-order finite strain theory [11]. Mineral adiabats were calculated [11] using an Anderson-Grüneisen parameter of 5.5 for all minerals except CaSiO₃ perovskite for which a value of 4.09 [6] was employed.

Calculation uncertainties

We can address the likely accuracy of our calculation of density and S velocity change (i.e. the impedance contrast) by considering equation [1] which is the basic reaction underlying the formation of CaSiO₃ perovskite. Using data in table 2 the volume change of equation [1] is calculated at 20.5 GPa to be -12.44 cm³/mol which is in excellent agreement with the thermodynamic assessment of equation [1] reported in equation [16] of -12560 J/GPa which is -12.56 cm³/mol. This corresponds to a density change of 6.7 % for equation [1] or 1 % in a peridotite and 2.1 % in MORB. The most uncertain parameter in the density calculation is the value of dKs/dT for CaSiO₃ perovskite. However if we assume an uncertainty of 30 % on the value of dKs/dT this affects the calculated density change for equation [1] by less than 3 %.

For S-wave velocity we calculate a change in Vs of 3.5 % for equation [1]. The largest uncertainty in this estimate is in the value of dG/dT for CaSiO₃ perovskite, which has never been experimentally measured but has been determined using ab initio calculations (6). If we consider this value to have an uncertainty of 30 %, then this propagates to an uncertainty in the ΔVs for equation [1] of 50 %. Therefore, given a very large increase in dG/dT, in line with a conservative estimate of the uncertainties, we would still expect a significant change in the shear velocity as a result of this reaction. We also point out that there are a number of literature estimates for the elastic properties of CaSiO₃ perovskite that would result in much larger values of ΔVs, e.g. [11].

The impedance contrast $\Delta\{\rho V_s\}$ of 1.5 % calculated for a peridotite assemblage has an uncertainty of ± 0.5 % if the 30 % uncertainties in dG/dT and dKs/dT are propagated.

Table S1. Starting garnet compositions

	Si	Al	Fe	Mg	Total
Peridotite	3.63	0.74	0.311	3.439	8
Basalt	3.3	1.4	0.274	3.026	8
Pyrope	3	2	0.249	2.751	8
Majorite	3.75	0.5	0.311	3.439	8

Table 1: Results

Garnet compositions in cations per 12 oxygen formula units									
Run No.	Pressure (GPa)	Si	Al	Fe	Mg	Ca	Total	Ring Fe/(Fe+Mg)	MW Fe/(Fe+Mg)
1600°C									
Pyrope									
S3550	19.2(3)	3.41(2)	1.08(4)	0.21(1)	2.25(6)	1.10(4)	8.050	0.626(3)	0.937641
S3549	19.9(2)	3.12(1)	1.52(2)	0.17(2)	2.25(5)	0.90(5)	8.038	0.542(3)	0.87(3)
S3470	18.8(5)	3.32(5)	1.36(4)	0.05(2)	2.03(8)	1.22(1)	7.993		
S3475	22.6(5)	3.11(6)	1.82(6)	0.207(6)	2.47(6)	0.37(3)	7.982		
S3478	23(5)	3.09(2)	1.77(3)	0.28(5)	2.56(6)	0.32(3)	8.023		
S3484	22.3(5)	3.08(5)	1.81(5)	0.24(7)	2.57(7)	0.30(7)	8.011	0.36(2)	
S3490	21.4(5)	3.10(5)	1.76(9)	0.23(1)	2.47(6)	0.44(1)	8.013		
Basalt									
S3551	20.4(3)	3.33(6)	1.11(7)	0.1(1)	2.94(8)	0.61(4)	8.096	0.496(2)	0.88(2)
S3550	19.2(3)	3.29(2)	1.36(4)	0.178(9)	1.90(6)	1.27(7)	8.023	0.626(3)	0.937641
S3549	19.9(2)	3.38(1)	1.14(3)	0.16(2)	2.70(3)	0.65(3)	8.044	0.542(3)	0.87(3)
S3548	19.5(2)	3.41(2)	1.04(3)	0.30(2)	2.56(3)	0.75(3)	8.068	0.605(5)	0.863(4)
S3547	19.5(5)	3.45(2)	1.04(2)	0.21(1)	2.58(5)	0.74(4)	8.020	0.592(2)	0.844(6)
S3764	21.2(3)	3.34(3)	1.26(2)	0.21(2)	2.85(6)	0.35(1)	8.021	0.426(5)	0.73(1)
S3757	20.7(5)	3.36(3)	1.29(4)	0.199(8)	2.65(3)	0.47(3)	7.990	0.469(2)	0.774(6)
S3783	22.3(2)	3.34(2)	1.31(2)	0.262(7)	2.81(4)	0.29(1)	8.010	0.350(4)	0.71(5)
S3657	19.9(3)	3.38(2)	1.01(5)	0.44(1)	2.62(5)	0.64(2)	8.108	0.545(3)	0.88(1)
S3655	19.9(5)	3.36(5)	1.25(7)	0.39(3)	2.40(6)	0.62(4)	8.018		
S3655	19.9(5)	3.42(1)	1.04(3)	0.24(3)	2.77(9)	0.58(2)	8.060		
S3460	18.5(5)	3.502(7)	1.06(2)	0.049(4)	2.22(6)	1.12(3)	7.970		
S3470	18.8(5)	3.44(2)	1.09(1)	0.03(7)	2.37(3)	1.05(2)	8.006		
S3478	23(5)	3.30(2)	1.33(3)	0.25(1)	2.89(6)	0.24(2)	8.028		
S3480	22.1(5)	3.47(5)	1.16(7)	0.27(2)	2.67(4)	0.37(3)	7.950	0.380(5)	
S3484	22.3(5)	3.33(3)	1.34(2)	0.20(6)	2.93(3)	0.188(7)	8.000	0.36(2)	
S3498	21.4(5)	3.33(5)	1.28(9)	0.276(8)	2.80(6)	0.34(3)	8.031	0.28(2)	
S3538	17.9(5)	3.33(5)	1.31(5)	0.20(2)	1.54(7)	1.62(6)	8.013		
Peridotite									
S3551	20.4(3)	3.54(4)	0.87(8)	0.26(3)	2.9(1)	0.44(8)	8.022	0.496(2)	0.88(2)
S3550	19.2(3)	3.62(2)	0.70(3)	0.22(8)	2.58(3)	0.92(3)	8.030	0.626(3)	0.937641
S3549	19.9(2)	3.58(1)	0.76(2)	0.11(4)	3.04(2)	0.54(2)	8.033	0.542(3)	0.87(3)
S3548	19.5(2)	3.61(1)	0.68(3)	0.23(2)	2.93(4)	0.59(3)8	8.051	0.605(5)	0.863(4)
S3547	19.5(5)	3.57(2)	0.77(3)	0.167(8)	2.88(5)	0.63(2)	8.037	0.592(2)	0.844(6)

S3764	21.2(3)	3.60(3)	0.80(2)	0.28(3)	3.02(2)	0.283(1)	8.000	0.426(5)	0.73(1)
S3757	20.7(5)	3.65(1)	0.69(1)	0.24(5)	3.082(4)	0.322(1)	7.998	0.469(2)	0.774(6)
S3784	23.5(4)	3.60(2)	0.68(9)	0.31(4)	3.4(1)	0.054(1)	8.061	0.545(3)	0.88(1)
S3460	18.5(5)	3.67(4)	0.63(3)	0.10(2)	2.79(7)	0.81(5)	8.010		
S3470	18.8(5)	3.664(3)	0.683(5)	0.05(2)	2.75(3)	0.84(3)	7.994		
S3475	22.6(5)	3.62(2)	0.791(2)	0.28(1)	3.21(5)	0.08(2)	7.984		
Majorite									
S3460	18.5(5)	3.78(4)	0.47(2)	0.098(9)	2.97(6)	0.65(4)	7.979		
S3470	18.8(5)	3.77(1)	0.49(1)	0.034(5)	2.87(7)	0.81(3)	7.985		
Reversals									
S3784	23.5(4)	3.15(1)	1.68(3)	0.26(2)	2.59(6)	0.30(4)	8.000	0.545(3)	0.88(1)
S3543	18.4(5)	3.39(6)	1.06(6)	0.17(3)	2.24(4)	1.21(5)	8.079		
S3515	19.8(5)	3.47(2)	1.05(2)	0.18(7)	2.59(3)	0.70(4)	8.000		
S3521	20.7(5)	3.55(4)	0.87(4)	0.33(2)	2.77(6)	0.48(4)	8.008		
S3523	20.8(5)	3.38(2)	1.20(3)	0.24(1)	2.64(2)	0.55(2)	8.015	0.464(3)	
1400°C									
Pyrope									
S3611	18.1(5)	3.17(3)	1.61(7)	0.144(7)	2.01(3)	1.08(5)	8.023		
S3614	18.6(5)	3.15(3)	1.56(5)	0.197(6)	2.09(6)	1.055(5)	8.064		
H2370	19.5(5)	3.10(6)	1.75(9)	0.236(5)	2.35(5)	0.58(4)	8.020	0.60(1)	0.93(1)
H2375	17.9(5)	3.24(1)	1.46(4)	0.200(5)	2.00(3)	1.11(3)	8.025		
H2241	19.6(5)	3.12(4)	1.76(6)	0.19(1)	2.41(5)	0.51(3)	7.996		
Basalt									
S3611	18.1(5)	3.301(8)	1.31(2)	0.199(4)	2.12(2)	1.11(2)	8.044		
S3614	18.6(5)	3.33(2)	1.17(4)	0.223(7)	2.49(2)	0.86(2)	8.080		
H2375	17.9(5)	3.40(3)	1.13(7)	0.223(8)	2.22(6)	1.04(3)	8.028		
Peridotite									
S3614	18.6(5)	3.56(1)	0.69(2)	0.263(7)	2.91(4)	0.66(4)	8.090		
S3611	18.1(5)	3.60(3)	0.71(5)	0.26(5)	2.68(4)	0.78(4)	8.042		

Notes: Ring and MW refer to ringwoodite and magnesiowustite molar Fe/(Fe+Mg) ratios of compositions in pressure calibration samples.

Table S3. Elasticity data

		V cm ³ / mol	α_0 (x10 ⁵)	α_1 (x10 ⁹)	α_2	K _{so} (GPa)	K'	dK _s /dT (GPaK ⁻¹)	G (GPa)	G'	dG/dT (GPaK ⁻¹)
Mg ₂ SiO ₄	Wad	40.51	2.85	3.20	0	170	4.3	-0.019	112	1.4	-0.017
Fe ₂ SiO ₄	Wad	43.15	2.32	7.12	-0.243	170	4.3	-0.019	72	1.4	-0.017
Mg ₂ SiO ₄	Ring	39.48	2.448	4.056	-0.6029	184	4.1	-0.021	121	1.3	-0.016
Fe ₂ SiO ₄	Ring	41.86	2.455	3.59	-0.3703	220	4.1	-0.021	96	1.3	-0.016
Mg ₄ Si ₄ O ₁₂	Garnet	113.88	2.87	2.89	-0.5443	166	4.2	-0.014	85	1.4	-0.0092
Mg ₃ Al ₂ Si ₃ O ₁₂	Garnet	113.19	2.87	2.89	-0.5443	171	3.2	-0.014	92	1.4	-0.0092
Ca ₃ Al ₂ Si ₃ O ₁₂	Garnet	125.31	2.87	2.89	-0.5443	166	5.4	-0.014	108.9	1.1	-0.0092
Fe ₃ Al ₂ Si ₃ O ₁₂	Garnet	115.44	1.78	1.21	-0.5071	174.9	4.7	-0.02	95.6	1.4	-0.0092
CaSiO ₃	Perov	27.45	3.22	6.88	0	236	4.5	-0.029	147	1.77	-0.0247

$$\alpha_1 = \alpha_0 + \alpha_1 T + \alpha_2 T^2 (\text{K}^{-1})$$

Table S4. Data source reference numbers for Table S3.

		α_0 (x10 ⁵)	α_1 (x10 ⁹)	α_2	K _o (GPa)	K'	dK/dT (GPaK ⁻¹)	G	G'	dG/dT
Mg ₂ SiO ₄	Wad	16	16	16	7	7	7	7	7	7
Fe ₂ SiO ₄	Wad	12	12	12	7	7	7	7	7	7
Mg ₂ SiO ₄	Ring	1	1	1	7	7	7	7	7	7
Fe ₂ SiO ₄	Ring	1	1	1	7	7	7	7	7	7
Mg ₄ Si ₄ O ₁₂	Garnet	*	*	*	8	8	*	8	8	*
Mg ₃ Al ₂ Si ₃ O ₁₂	Garnet	9	9	9	20	20	10	20	20	10
Ca ₃ Al ₂ Si ₃ O ₁₂	Garnet	*	*	*	20	20	*	20	20	*
Fe ₃ Al ₂ Si ₃ O ₁₂	Garnet	14	14	14	18	18	17	17	17	*
CaSiO ₃	Perov	6	6	6	6	6	6	6	6	6

* indicates that the same values as for pyrope have been employed.

Additional References to the supporting data

1. K. Matsuzaka, M. Akaogi, T. Suzuki, T. Suda, *Phys. Chem. Minerals*, **27**, 310 (2000).
2. D. J. Frost, F. Langenhorst, P van Aken, *Phys. Chem. Minerals*, **28**, 455 (2001).
3. D. J. Frost, *Earth. Planet. Sci. Lett.* **216**, 313 (2003).
4. D. J. Frost, *Am. Mineral.*, **88** 387 (2003).
5. H. St. C. O'Neill, B. J. Wood, *Contrib. Mineral. Petrol.* **70**, 59 (1979).
6. L. Li, D. J. Weidner, J. Brodholt, D. Alfè, G. D. Price, R. Caracas, R. Wentzcovitch, *Phys. Earth. Planet. Int.* **155**, 249 (2006).
7. S. V. Sinogeikin, J. D. Bass, T. Katsura, *Phys. Earth. Planet. Int.* **136**, 41 (2003).
8. S. V. Sinogeikin, J. D. Bass, *Geophys. Res. Lett.* **29**, 10.1029/2001GL013937 (2001).
9. M. Akaogi, A. Tanaka, E. Ito, *Phys. Earth. Planet. Int.* **132**, 303 (2002).
10. S. V. Sinogeikin, J. D. Bass, *Earth. Planet. Sci. Lett.* **203**, 549 (2002).
11. F. Cammarano, S. Goes, P. Vacher, D. Giardini, *Phys. Earth. Planet. Int.* **138**, 197 (2003).
12. Y. Fei, H-K. Mao, B. O. Mysen, *J. Geophys. Res.* **96**, 2157 (1991).
13. Y. Sato, in *High Pressure Research in Geophysics* (Academic Press, New York 1977), pp 307-324.
14. B. J. Skinner, in *Hand Book of Physical Constants* (Geol. Soc. Am. Mem. 1966) pp. 75-95.
15. B.Li, R. C. Liebermann, D. J. Weidner, *Science* **281**, 675-677.
16. I. Jackson, S. M. Rigden, *Phys. Earth. Planet. Int.* **96**, 85 (1996).
17. F. Jiang, S. Speziale, T. S. Duffy, *J. Geophys. Res.* **109**, 10.1029/2004JB003081 (2004).
18. M. Akaogi, N. Ohmure, T. Suzuki, *Phys. Earth. Planet. Int.* **106**, 103 (1998).
19. Y. Meng, Y. Fei, D. J. Weidner, G.D. Gwanmesia, J. Hu, *Phys. Chem. Mineral* **21**, 407 (1994).
20. P.G. Conrad, C-S. Zha, H-K. Mao, R. J. Hemley, *Am. Mineral.* **84**, 374 (1999).